Brick comparison of in-medium energy loss models

Marta Verweij, Marco van Leeuwen

Partons traversing a strongly interacting medium lose energy, dominantly due to gluon radiation. The energy loss of partons in a strongly interacting medium has been described by phenomenologically different models. We study the TECHQM brick problem by comparing brick calculations of the multiple soft approximation with the opacity expansion approximation. The gluon emission distributions and energy loss probability distributions are compared. An approximation of the nuclear modification factor R_{AA} is calculated. For a given suppression factor different initial bulk conditions in terms of temperature T (or transport coefficient $\hat{q}$) and parton path length L are needed for the different energy loss mechanisms.

The multiple soft scattering approximation is compared with the opacity expansion formalism. For this work we used the following energy loss models:

- **Salgado-Wiedemann multiple soft scattering** (ASW-BDMPS) [1].
- **Salgado-Wiedemann Opacity Expansion** (SWOE): The single hard scattering approximation as described in [1]. It consists of an incoherent superposition of a few single hard scatterings. Originally with a fixed value for L/λ. For this work L/λ is calculated from the temperature T in the medium.
- **Wicks-Horowitz-Djordjevic-Gyulassy Opacity Expansion** (WHDG)[2]: this model is based on the GLV opacity expansion [3] and calculates the radiated gluon energy starting from an analytical expression for the single gluon emission spectrum to all orders of opacity. For the single gluon spectrum there is a cut-off given by the parton energy. Using the average number of emitted gluons the $P(\Delta E)$ is calculated for a parton. The energy loss is calculated following the DGLV formulas for radiative energy loss as reported in appendix B of [2] (WHDG).

1 Common scale T

The multiple soft scattering approximation and the opacity expansions calculate a energy loss probability distribution which consists of a discrete part p_0 indicating the probability to lose no energy and a continuous part $p(\Delta E)$ caused by emission of one or more gluons:

$$P(\Delta E; R, \omega_c) = p_0(R)\delta(\Delta E) + p(\Delta E; R, \omega_c). \quad (1)$$

The quenching weights provided by [1] are used to calculate the energy loss in the BDMPS formalism. The quenching weights are a function of the characteristic gluon energy ω_c and the kinematical constraint R:

$$\omega_c = \frac{1}{2}\hat{q}L^2, \tag{2}$$

$$R = \frac{2\omega_c^2}{\hat{q}L} = \omega_c L = \frac{1}{2}\hat{q}L^3, \tag{3}$$

in which the transport coefficient $\hat{q}$ is defined as

$$\hat{q} = \frac{\langle k_t^2 \rangle}{\lambda} = \frac{72 \cdot 1.202\alpha_s^2}{\pi} T^3. \tag{4}$$

The input parameters for the calculation the quenching weights for the opacity expansions are the pQCD color screening mass μ, in-medium path length L and the number of scattering centers $\frac{1}{\lambda}$:

$$\mu = \sqrt{4\pi\alpha_s} T \tag{5}$$

$$\frac{1}{\lambda} = \rho\sigma = \frac{144 \cdot 1.202\alpha_s}{8\pi^2} T \tag{6}$$

For the single hard scattering approximation the following input parameters are used:

$$\bar{\omega}_c = \frac{1}{2}\mu^2 L = 2\pi\alpha_s T^2 L, \tag{7}$$

and analogously to the BDMPS formalism the kinematic constraint:

$$\bar{R} = \bar{\omega}_c L = 2\pi\alpha_s T^2 L^2. \tag{8}$$

Note that $\bar{\omega}_c$ is not the same as ω_c in the BDMPS approximation and that the energy loss in the single hard scattering approximation scales with:

$$\Delta E \propto \frac{L}{\lambda}\bar{\omega}_c = \frac{1}{2}\hat{q}L^2 = \omega_c \tag{9}$$

All the input parameters as defined for the BDMPS formalism and opacity expansions depend on temperature T which makes it possible to make a direct comparison between the phenomenologically different models.

2 Brick results

In order to understand better the differences between the energy loss calculation of the BDMPS formalism and the opacity expansion approach, calculations are done with a uniform medium and fixed path length L. Although this is not a realistic scenario for a heavy ion collision it will give insight into the differences between different energy loss models.

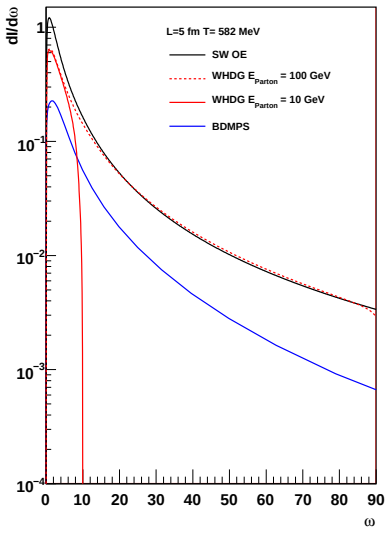

(a) Comparison of single gluon spectra for different energy loss formalisms. This is for a static uniform medium with $T = 582$ MeV and path length $L = 5$ fm.

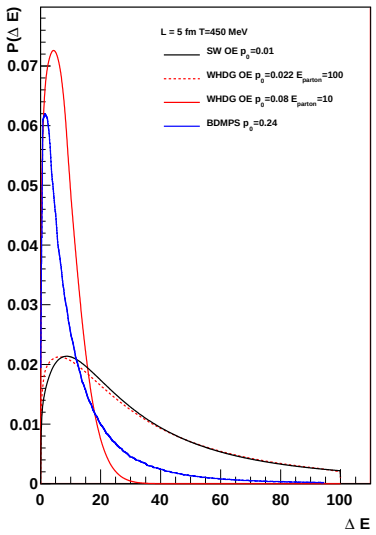

(b) Energy loss probability distributions for the different models. The continuous part of the probability distribution in equation 1 is shown as function of the energy loss ΔE and the discrete weights p_0 are reported in the legend for each model. This is for a static uniform medium with $T = 450$ MeV and path length $L = 5$ fm.

Figure 1: Comparison of gluon spectra and energy loss probability functions for different models for two different bricks.

There are differences between the gluon radiation of an in-medium produced parton for the different models. The single gluon radiation spectra are shown in figure 1(a). From these spectra the average number of emitted gluons can be obtained by integrating the gluon spectrum over the gluon energy ω:

$$\langle N_{gl} \rangle = \int d\omega \frac{dI}{d\omega}. \tag{10}$$

And the average energy loss per radiated gluon can be calculated as follows:

$$\langle \omega \rangle = \frac{\int d\omega \; \omega \frac{dI}{d\omega}}{\langle N_{gl} \rangle}. \tag{11}$$

The obtained values for a brick with medium conditions as in figure 1(a) ($L = 5$ fm and $T = 582$ MeV) are given in the first two columns of table 1. If the cut-off in the single gluon energy spectrum for the WHDG model is set to a large value ($E_{parton} = 100$ GeV) it approximates the Salgado-Wiedemann single hard scattering approximation (SWOE) in case the temperature T and in-medium path length are not too small ($L \geq 5$ fm and $T \geq 250$ MeV). Note that the gluon spectrum labeled by SWOE is multiplied with the corresponding value of L/λ depending on the temperature of the medium. The total energy loss, $\langle N_{gl} \rangle \langle \omega \rangle$, in the BDMPS formalism is smaller than the two opacity expansions (WHDG with $E_{parton} = 100$ GeV and SWOE).

In figure 1(b) the energy loss probability distribution is shown for a fixed path length $L = 5$ fm and a medium temperature $T = 450$ MeV. The probability for a parton to lose no energy, the discrete weight p_0, under these specific medium conditions is given in the legend of the figure. In the BDMPS formalism the discrete weight is much larger (0.24 for BDMPS and $0.01 - 0.08$ for the opacity expansions). This is also reflected in table 1 by the smaller number of average emitted gluons in BDMPS which defines the discrete weight to $p_0 = e^{-\langle N_{gl} \rangle}$. The tail at $\Delta E > 20$ GeV of the continuous weights is much more significant for SWOE and WHDG with $E_{parton} = 100$ GeV than in the BDMPS formalism. However for RHIC energies this will not be very important because a typical jet energy is ≈ 10 GeV. The parton loses on average more energy in the WHDG($E_{part} = 100$ GeV) and SWOE formalism compared to the BDMPS formalism under the same medium conditions. The average energy loss $\langle \Delta E \rangle$ for a parton with $E = 10$ GeV corresponding to the $P(\Delta E)$ distributions from figure 1(b) (see table 1) is much smaller for the BDMPS formalism than for the opacity expansion.

	$\langle N_{gl} \rangle$	$\langle \omega \rangle$ (GeV)	$\langle \Delta E \rangle$ (GeV)	R_8
BDMPS	2.0	13	3.4	0.13
WHDG (E=10 GeV)	3.0	3.2	5.4	$5.6 \cdot 10^{-3}$
WHDG (E=100 GeV)	5.3	12	8.1	$5.3 \cdot 10^{-2}$
SWOE	7.2	9.8	9.0	$7.7 \cdot 10^{-4}$

Table 1: Average number of gluons $\langle N_{gl} \rangle$, average energy loss per gluon $\langle \omega \rangle$ corresponding to figure 1(a). The average energy loss $\langle \Delta E \rangle$ and R_8 are calculated from the energy loss probability distribution $P(\Delta E)$ with $\Delta E_{max} = 10$ GeV. All the reported numbers are for a brick of $L = 5$ fm and $T = 582$ MeV

The nuclear modification factor R_{AA} can be approximated by the weighted average energy loss:

$$R_n = \int_0^1 d\epsilon (1-\epsilon)^n P(\epsilon), \tag{12}$$

in which $\epsilon = \Delta E/E$ and n is the power of the p_t spectrum of the measured hadrons. Because for RHIC energies the p_t distribution is very similar to a power law spectrum with $n = 8$, R_8 will be used as an approximation for R_{AA}. In the last column of table 1 the R_8 values for the specific brick of $L = 5$ fm and $T = 582$ MeV. Again we see that in the opacity expansion formalism the suppression is larger than in the BDMPS formalism. In figure 2 R_8 is shown

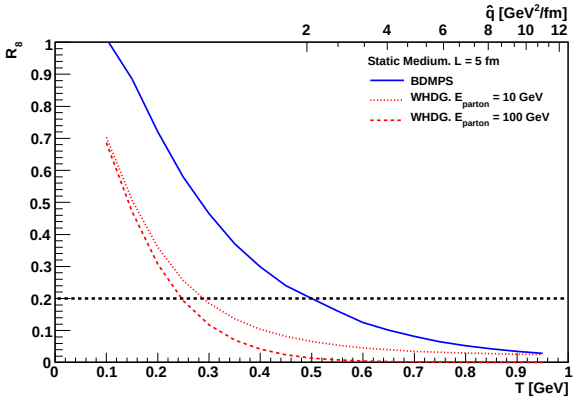

Figure 2: R_8 as function of medium temperature T for a static uniform medium. The thickness of the medium is fixed at $L = 5$ fm. The black dashed line represents $R_8 = 0.2$. R_8 has been calculated with $E = 10$ GeV in $\epsilon = \Delta E/E$.

as function of medium temperature for a static uniform medium and a fixed medium thickness of $L = 5$ fm. RHIC data have shown that for the high p_t region R_{AA} has a constant value of approximately 0.2 [4, 5, 6]. A R_8 value of 0.2 is reached at $T = 260$ MeV for WHDG with the single gluon energy cut-off of 10 GeV, at $T = 290$ MeV for WHDG with a cut-off on the single gluon energy of 100 GeV and $T = 500$ MeV for BDMPS. We will focus on the differences between BDMPS and WHDG ($E_{parton} = 100$ GeV).

The temperature is not the only property of the medium which influences the energy loss of a parton traversing a hot dense medium. Another important property is the thickness of the medium which in figures 1 and 2 is fixed at $L = 5$ fm. Figure 3(a) shows contours of L and T for a fixed constant value of $R_8 = 0.2$. The energy loss of a parton increases if the temperature T is larger or if the path length L in the medium is longer. Clearly the differences in temperature for the various opacity expansions is small compared to the difference with BDMPS. We visualize the differences in required length and temperature for BDMPS and WHDG by taking the ratio of them. In the the upper panel of figure 3(b) T_{BDMPS}/T_{WHDG} is shown as function of L and the

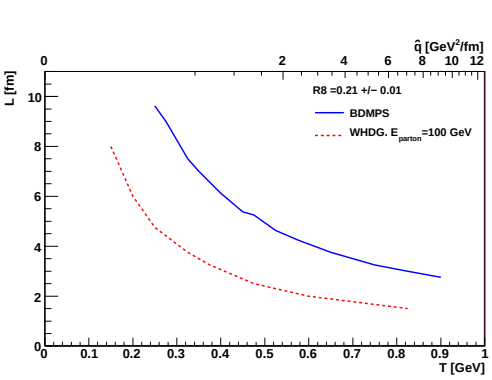

(a) Medium temperature T versus thickness L for a static medium for $0.2 < R_8 < 0.22$.

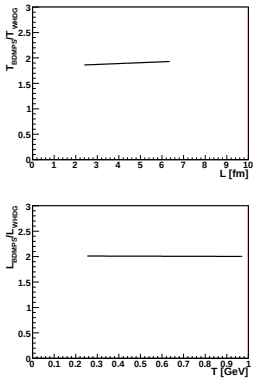

(b) Upper panel: T_{BDMPS}/T_{WHDG} as function of length L for $R_8 = 0.21$. Lower panel: L_{BDMPS}/L_{WHDG} as function of temperature T for $R_8 = 0.21$.

Figure 3: Mapping of energy loss formalisms BDMPS and WHDG in length L and temperature T.

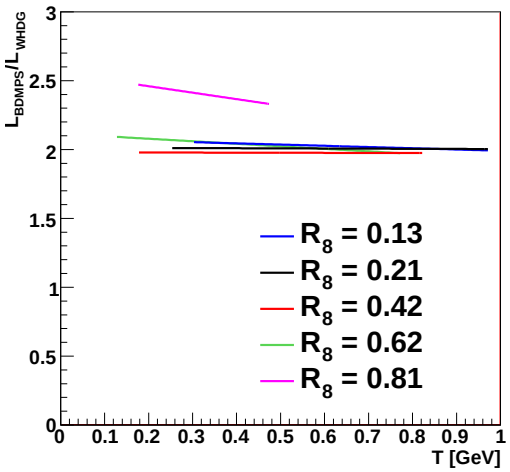

Figure 4: L_{BDMPS}/L_{WHDG} as function of temperature T for different values of R_8.

lower panel shows L_{BDMPS}/L_{WHDG} as function of T. It turns out that a simple translation can be made between the BDMPS and the WHDG opacity expansion

formalism. A mapping in L seems to be more universal than a mapping in T. For the same value of R_8 and the same medium temperature the in-medium path length in the BDMPS formalism is approximately twice as large as in the WHDG opacity expansion formalism: $L_{BDMPS}/L_{WHDG} \approx 2$. This mapping in L holds for $0.1 < R_8 < 0.6$. In figure 4 L_{BDMPS}/L_{WHDG} is shown as function of temperature for different values of R_8. It is remarkable that over a wide range of temperature T and R_8 a constant conversion factor between the two phenomenologically different models can be found.

To further compare the energy loss mechanisms with a mapping in L in figure 5 for both models (BDMPS and WHDG) $P(\Delta E)$ is shown with $L = 2$ fm (figure 5(a)) and $L = 5$ fm (figure 5(b)). The distributions for WHDG (red dotted line) and BDMPS with $L' = 1.9L$ (black dotted line) are very similar for the case $L = 5$ fm, see figure 5(b). In the tail of the distribution with $L = 2$ fm, figure 5(a), the black line for BDMPS with $L' = 1.9L$ starts to deviate. However for the relevant region $\Delta E < 20$ GeV for small in-medium path lengths the black and red dotted lines (WHDG) correspond very well.

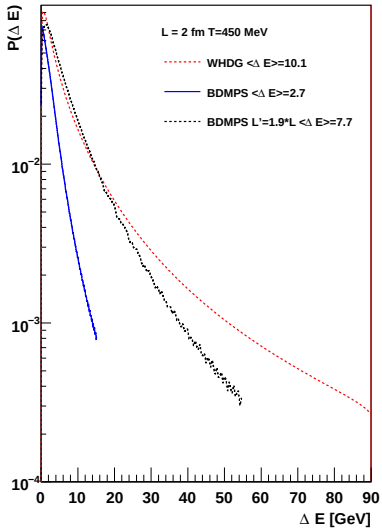

(a) Energy loss probability distributions for the different models: WHDG with $T = 450$ MeV, $L = 2$ fm and BDMPS with $T = 450$ MeV and $L = 2$ fm and $L' = 1.9L$.

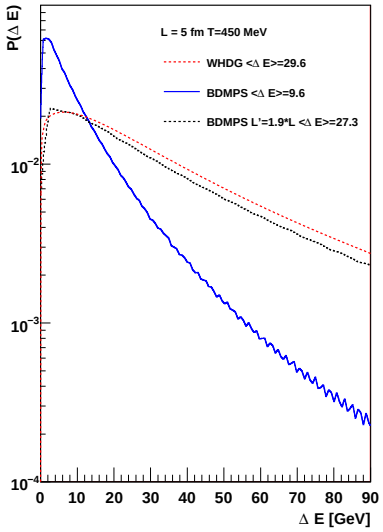

(b) Energy loss probability distributions for the different models: WHDG with $T = 450$ MeV, $L = 5$ fm and BDMPS with $T = 450$ MeV and $L = 5$ fm and $L' = 1.9L$.

Figure 5: Energy loss probability distributions for different medium thicknesses.

To summarize the contours for a brick which results in $R_8 = 0.1$, 0.2 and 0.4 are shown in figure 6 as a function of the $\hat{q}$ and L. In case of WHDG the

transport coefficient is defined as

$$\hat{q} = 2\bar{w}_c \frac{L}{\lambda}/L^2 = \frac{\mu^2}{\lambda}, \tag{13}$$

which is the exact definition of $\hat{q}$ in the multiple soft scattering approximation. A relatively small difference in L results in a very large difference in $\hat{q}$ for a fixed value of R_8. We already showed that the models can be mapped by a simple scaling factor of ≈ 2 in path length L. This is because a scaling in L is much more efficient than a scaling in medium density because the energy loss scales with $\hat{q}L^2$. To achieve a significant difference in the fraction of energy that is lost a large difference in medium density is needed.

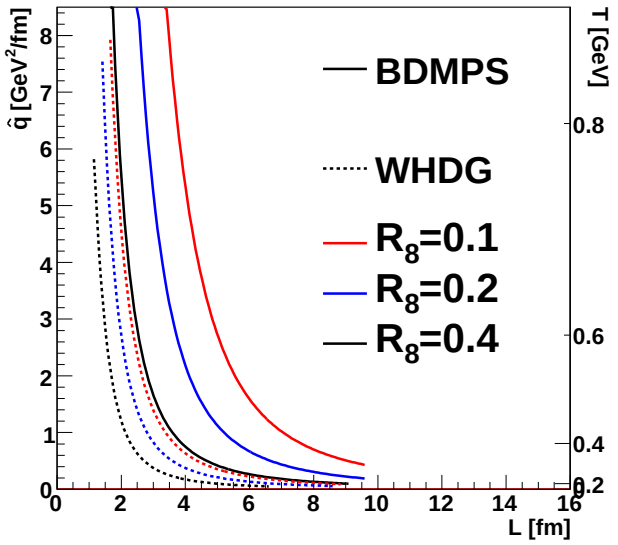

Figure 6: In-medium path length versus transport coefficient for BDMPS (solid lines) and WHDG (dotted lines) energy loss models. The lines represent isolines from brick calculations for $R_8 = 0.1$ (red), 0.2 (blue) and 0.4 (black).

3 Discussion

In this analysis the energy loss calculations in the multiple soft scattering approximation and the opacity expansion for a fixed path length and homogeneous medium are compared. The input parameters to calculate the energy loss in both models are defined in the same way and depend on T and L. The energy loss in the opacity expansion is significantly larger than in the multiple soft scattering approximations under the same medium conditions. For example

the same suppression factor in terms of $R_8 = 0.2$, see equation 12, with fixed path length $L = 5$ fm is found at $T = 260$ MeV for the WHDG in the limit of infinite maximal single gluon emission energy and at $T = 500$ MeV for the ASW-BDMPS model.

The WHDG model with $E_{parton} \to \infty$ gives similar results as the ASW single hard approximation (SWOE). The larger energy loss in the opacity expansion formalism is mainly caused by the smaller values for the discrete weight of the energy loss probability distribution.

The large differences in necessary temperature in order to obtain the same suppression seems to be equal to a mapping in L: $L_{BDMPS}/L_{WHDG} \approx 2$. If the length of the brick in the BDMPS calculation is twice as long as in the WHDG calculation the nuclear modification factor R_8 is the same as function of temperature. Since the transport coefficient $\hat{q}$ is very steep for a given R_8 as function of L this mapping in L is equivalent to a very large difference in temperature or transport coefficient $\hat{q}$ as is shown in figure 6. It is not yet clear which assumptions in the energy loss models cause the sizable differences in the predicted suppression.

References

[1] C.A. Salgado, U.A. Wiedemann, Phys. Rev. **D68**, 014008 (2003), `hep-ph/0302184`

[2] S. Wicks, W. Horowitz, M. Djordjevic, M. Gyulassy, Nucl. Phys. **A784**, 426 (2007), `nucl-th/0512076`

[3] M. Gyulassy, P. Levai, I. Vitev, Nucl. Phys. **B571**, 197 (2000), `hep-ph/9907461`

[4] J. Adams et al. (STAR), Phys. Rev. Lett. **91**, 172302 (2003), `nucl-ex/0305015`

[5] S.S. Adler et al. (PHENIX), Phys. Rev. Lett. **91**, 072301 (2003), `nucl-ex/0304022`

[6] S.S. Adler et al. (PHENIX), Phys. Rev. **C69**, 034910 (2004), `nucl-ex/0308006`